DNA-Based Molecular Wires: Multiple Emission Pathways of Individual Constructs

Gabriel Sánchez-Mosteiro,[†,‡] Erik M. H. P. van Dijk,[†] Jordi Hernando,[||] Mike Heilemann,[⊥] Philip Tinnefeld,[¶] Markus Sauer,[¶] Felix Koberlin,[#] Matthias Patting,[#] Michael Wahl,[#] Rainer Erdmann,[#] Niek F. van Hulst,[‡,§] and Maria F. García-Parajó*[,§,£]

Applied Optics Group, Faculty of Science and Technology and MESA+ Institute for Nanotechnology, University of Twente, P. O. Box 217, 7500 AE Enschede, The Netherlands, ICFO—Institut de Ciències Fotòniques, 08860 Castelldefels, Spain, ICREA—Institució Catalana de Recerca i Estudis Avançats, 08015 Barcelona, Spain, Departament de Química, Universitat Autònoma de Barcelona, 08193 Cerdanyola del Vallès, Spain, Clarendon Laboratory, Department of Physics, University of Oxford, Parks Road, Oxford OX1 3PU, United Kingdom, Applied Laser Physics and Laser Spectroscopy, Faculty of Physics, University of Bielefeld, Universitätsstr. 25, 33615 Bielefeld, Germany, PicoQuant GmbH, Rudower Chaussee 29, 12489 Berlin, Germany, and Laboratory of NanoBioengineering, Barcelona Science Park (PCB), Josep Samitier 1−5, 08028 Barcelona, Spain

Received: July 24, 2006; In Final Form: September 19, 2006

The extent of photon energy transfer through individual DNA-based molecular wires composed of five dyes is investigated at the single molecular level. Combining single-molecule spectroscopy and pulse interleaved excitation imaging, we have directly resolved the time evolution spectral response of individual constructs, while simultaneously probing DNA integrity. Our data clearly show that intact wires exhibit photon-transfer efficiencies close to 100% across five dyes. Dynamical and multiple pathways for the photon emission resulting from conformational freedom of the wire are readily uncovered. These results provide the basis for guiding the synthesis of DNA-based supramolecular arrays with improved photon transport at the nanometer scale.

Introduction

During the past decade much research attention has been devoted to the design and synthesis of supramolecular structures of precise length, geometry, and composition in view of their potential application for molecular-based electronics and photonics. In particular, organic fluorescent molecules are currently being explored as building blocks for "bottom-up" design of molecular switches,[1] optoelectronic gates,[2] light-driven molecular motors,[3] and photonic wires.[2] In parallel, the advent of single-molecule detection in complex environments and at room temperature has already allowed investigation at the individual level of a first generation of potential photonic devices.[4−6] For instance, controlled "on−off" photon switching at the individual level has been demonstrated by Irie et al.[4a] and more recently by Heilemann et al.[4b] and Habuchi et al.[4c] Similarly, molecular photonic wires based on one-dimensional multichromophoric arrays have been designed and studied at the single molecular level.[6−8] These first experiments have successfully proved that light can be absorbed and transported along well-defined molecular architectures with high efficiency but have also revealed their complex photophysical behavior. Detailed understanding of the multiple pathways for photon emission in these systems might guide the rational design of improved molecular arrays for efficient collection and unidirectional transport of light at the nanometer scale.

Molecular photonic wires rely on the transport of excited-state energy from an absorption site toward the other end of the assembly, where the energy can be released by photon emission.[2] Most of the work reported so far is based on porphyrins as building blocks[2,9] or a combination of perylene−porphyrin assemblies with different size linkers.[10] Although highly efficient, these arrays are sensitive to electronic interactions and excimer formation which eventually result in energy sinks that interrupt the energy flow along the wire. Long one-dimensional perylene pendant polyisocyanide polymers have been also synthesized and investigated at the individual molecular level.[8] Despite the very-well-defined geometry, accurate distance between consecutive perylenes, and polymer rigidity, their optical properties are again dominated by intramolecular excimer-like emission.[8]

An alternative route toward the design of molecular photonic wires is provided by the use of DNA as scaffold for the accurate attachment of chromophores, allowing in principle the design of long one-dimensional arrays. With a persistence length of 50 nm, DNA constitutes a stiff scaffold for the chromophores.[11] In addition, well-developed labeling strategies allow selective attachment of fluorophores at controlled distances and with distinct excited-state properties. For instance, cooperative perylene assembly on the minor grove of the DNA has been successfully demonstrated.[12] Using sequential hybridization of short single-stranded oligonucleotides labeled with fluorophores, Vyawahare et al. demonstrated a combination of homo- and hetero-Förster-type energy transfer (FRET) through DNA wires composed of five dyes.[13] The overall ensemble transfer efficiency was estimated to be 9%. Recently, we reported a similar DNA-based scheme with five different dyes and demonstrated FRET efficiencies of 90% on individual DNA−molecular wires at the single-molecule level.[7] Unfortunately, only 10% of

* To whom correspondence should be addressed at Barcelona Scientific Park. E-mail: mgarcia@pcb.ub.es.
[†] University of Twente.
[‡] ICFO.
[§] ICREA.
[||] Universitat Autònoma de Barcelona.
[⊥] University of Oxford.
[¶] University of Bielefeld.
[#] PicoQuant GmbH.
[£] PCB.

10.1021/jp064701f CCC: $33.50
Published on Web 12/05/2006

photonic wires exhibited photon emission until the last dye. Moreover, their emission was accompanied by a rather complex and dynamical fluorescence behavior.

In here we report on the combination of single-molecule spectroscopy (SMS) with pulse interleaved excitation imaging[14] to thoroughly investigate the extent of photon energy transfer on individual wires. Using these techniques, we have disentangled the intricate relationship between energy transfer, sinks, and leakages on individual constructs. Our data clearly show multiple pathways for the photon emission, a phenomenon that most probably results from conformational freedom and partial DNA hybridization on these complex systems.

Experimental Methods

Single-stranded DNA fragments with attached chromophores via C6 amino linkers were purchased from IBA GmbH. Rhodamine green (RhG) was attached to the modified 5′ end of a 60 base pair (bp) single-stranded DNA fragment. Tetramethylrhodamine (TMR), ATTO590, ATTO620, and ATTO680 were attached to three different 20bp single-stranded DNA fragments complementary to the 60bp single-stranded fragment of the RhG. Hybridization of the labeled single-stranded DNA fragments to form a double-stranded DNA was performed by heating a solution containing all the fragments in phosphate-buffered saline (PBS, pH 7.4) to 363 K (25 μL of each single strand of 5×10^{-5} M concentration was mixed in a 2 mL vial), keeping the temperature constant for 10 min followed by a slow cooling to room temperature for 6 h (PTC-150 MiniCycler, MJ Research). All bulk and single-molecule experiments were performed on five-dye DNA constructs.

Bulk steady-state measurements were performed on solutions of DNA wires composed in principle of five dyes (50 nM) on PBS. Absorption spectra were measured on a Shimadzu UV-VS2101PC spectrophotometer. Fluorescence spectra were recorded on a Cary Eclipse fluoro-spectrophotometer. Bulk fluorescence emission spectra were recorded with $\lambda_{exc} = 468$ nm, and excitation spectra, recorded at $\lambda_{det} = 703$ nm.

Samples for the single-molecule measurements were prepared by spin coating solutions of DNA wires ($\sim 10^{-9}$ M) in PBS on a cover glass at 2800 rpm for 50 s. The cover glasses were cleaned by means of an O_2-etching plasma treatment for 5 min immediately before sample preparation. Only freshly prepared samples were used in the single-molecule experiments.

Single-molecule experiments were carried out using a confocal scanning fluorescence microscope (CFM, Zeiss Axiovert inverted microscope) with an oil-immersion objective lens (Olympus NA 1.4, 100×).[15] Circularly polarized light ($\lambda_{exc} =$ 468 nm, picosecond laser diode LDH470, PicoQuant, 3 kW/cm^2) was used to excite the samples. A band-pass excitation blocking filter was inserted at the entrance of the microscope (470FS10-25, Andover Co.). The fluorescence light emitted by individual wires was collected through the same objective lens and separated from the excitation light by the combination of a dichroic mirror (Omega 515DRLP) and a long pass filter (Omega 500ALP). 50% of the fluorescence light was then sent to two avalanche photodiodes (APD, SPCM-AQ-14, EG&G Electro Optics) while the remaining 50% of the fluorescence light was sent toward a CCD camera (Andor, DV437−BV) for single-molecule spectra recording. A dichroic beam splitter (Omega 585DRLP) in front of the APDs splits the light into two different spectral windows (above and below 585 nm). A direct-vision prism in front of the CCD camera spreads the fluorescence light into its wavelength components. Fluorescence trajectories were recorded at 1 ms integration time, while fluorescence spectra was collected with 1 s integration time. The whole setup was computer-controlled by custom-made Labview software.

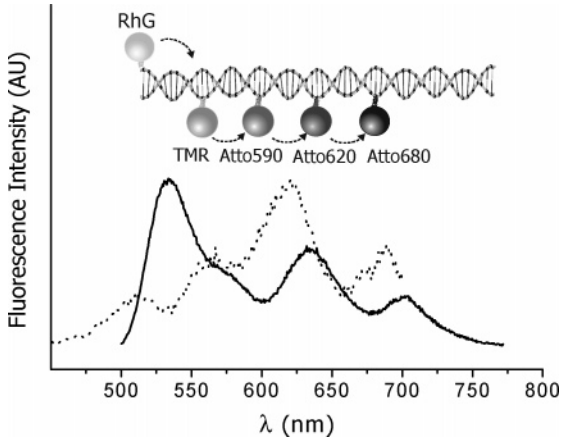

Figure 1. (Inset) Cartoon of the molecular photonic wire. Five distinct chromophores are covalently attached to ssDNA fragments and hybridized to a ds60bp DNA construct. Bulk fluorescence emission spectrum ($\lambda_{exc} = 468$ nm, straight line) and excitation spectrum ($\lambda_{coll} = 703$ nm, dotted line) of a 50 nM solution of DNA wires.

Pulsed interleaved excitation (PIE) experiments were performed on a time-resolved CFM MicroTime200 (PicoQuant).[16] Two pulsed lasers ($\lambda_{exc} = 468$ nm (blue), picosecond laser diode head LDH470, PicoQuant; and $\lambda_{exc} = 635$ nm (red), picosecond laser diode head LDH-635, PicoQuant) were used as excitation sources (~1 kW/cm^2, 90 ps fwhm, 10 MHz). Blue and red pulses were delayed by 50 ns with respect to each other to ensure that each detected photon could be related to its excitation pulse. The light was focused on the sample using a water-immersion objective (Zeiss, C-apochromat, NA 1.2, 63×). The fluorescence was collected through the same objective and split into two spectral windows using a dichroic beam splitter (640DCXR, AHF analysentechnik) and band-pass filters in front of each detector (HQ545/100 AHF analysentechnik for the "blue" detector and HQ685/70 AHF analysentechnik, for the "red" detector). The fluorescence photons were detected using avalanche photodiodes (SPCM-AQR-14, EG&G, Optoelectronics) and recorded using a time-correlated single-photon counting card (TimeHarp200, PicoQuant). Three sets of images (8 μm^2) were obtained in each experiment, i.e., blue excitation−blue detection, blue excitation−red detection, and red excitation−red detection. Images were analyzed using custom-written Labview-based software.

Results and Discussion

Figure 1 (inset) shows a cartoon of our system. Five different chromophores are covalently attached to a double-stranded helix of DNA by means of C6-amino linkers and spaced by 10bp corresponding to an interchromophoric distance of ~3.4 nm and a total length of 13.6 nm. The chromophores (RhG, TMR, ATTO590, ATTO620, and ATTO680) were selected in such a way that the emission spectrum of each chromophore overlaps the absorption spectrum of its neighbor, creating an energy cascade with a spectral range of ~200 nm. Taking into account the small distances involved, the spectral overlap between consecutive emission spectra of donors and absorption spectra of acceptors, and assuming full rotational freedom of the chromophores ($k^2 = 2/3$), a highly efficient FRET process between consecutive dyes is expected (FRET > 98% in each step) and an overall FRET efficiency of ~95% for the full constructs.

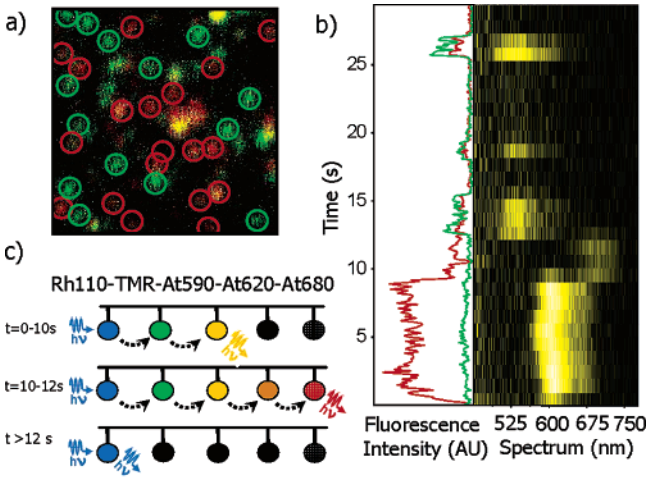

Figure 2. (a) Pseudo-color-coded fluorescence image ($10 \times 10\ \mu m^2$) of individual DNA molecular photonic wires. The green and red spots correspond to emission below and above 585 nm, respectively. (b) Simultaneously recorded fluorescence intensity time trace and 2D spectra trace of an individual DNA molecular photonic wire. (c) Cartoon illustrating the different stages on the emission of this particular molecular photonic wire.

Both bulk excitation and emission spectra at low concentration solutions (50 nM) are shown in Figure 1, confirming FRET until the last dye. Fitting the bulk emission spectra to a linear combination of the emission spectra of the individual chromophores yields the number of photons emitted from every dye. We then define the emission efficiency from the wire (E_{wire}) as the ratio between the intensity emitted from the last dye (ATTO680) over the total intensity of the wire. This results in a $E_{wire} \sim 14\%$ for this particular hybridization. This is in contrast to $E_{wire} \sim 87\%$, as expected by taking into consideration the FRET efficiency for every step and the quantum yield, φ, of the individual dyes. The discrepancy between experimental and calculated values, and the rather low experimental E_{wire} obtained, are consistent with data from Vyawahare et al.[13] and recent work from Heilemann et al.[7] Moreover, we found variations in E_{wire} from different hybridization experiments, suggesting that hybridization is not 100% reproducible.

To investigate the origin for the low FRET efficiencies obtained in bulk measurements, we performed single-molecule experiments on diluted solutions of the constructs (10^{-9} M in PBS) spin-coated onto a glass substrate. Individual photonic DNA wires were excited with circularly polarized light at $\lambda = 468$ nm and the emission fluorescence light collected using a home-built confocal scanning optical microscope allowing simultaneous detection of the fluorescence intensity together with spectral measurements (see Experimental Section for details).

Figure 2a shows a pseudo-color-coded image ($10 \times 10\ \mu m^2$) of individual wires. The green spots correspond to fluorescence photons emitted mainly from the first dye (RhG, ~70%) and some contribution from TMR (~30%), while the red spots correspond to fluorescence emitted from the other chromophores composing the wire. From this and other similar images we found that 52% of the wires emit above 585 nm. Brighter spots, most probably corresponding to multiple DNA wires within the excitation volume, were excluded from the analysis. To directly investigate the spectral response of individual wires, we followed their time evolution spectra simultaneously with its fluorescence intensity. Figure 2b shows a typical intensity time trace (left) together with its corresponding 2D spectra trace (right). Both spectra and time-dependent fluorescence intensity trajectories reflect the evolution of the fluorophoric system as a function of time and reveal a rather complex photophysical behavior. Hence, during the first 10 s of the trajectories, the fluorescence is dominated by emission of the third and fourth dyes, as inferred from the 2D spectra. At $t = 10$ s the last dye partially recovers the emission, as seen from the appearance of a peak on the spectrum at ~700 nm and a decrease of the intensity ($\varphi = 0.3$ for the last dye, while $\varphi = 0.8$ for the third and fourth dyes). During 10 s $< t <$ 12 s, one is able to recover a FRET ~ 100% to the last dye. From $t >$ 12 s the fluorescence is dominated by emission from the first dye and interrupted by long dark periods. The cartoon in Figure 2c illustrates the overall observed behavior for this particular wire. Remarkably, the time evolution of the fluorescence trajectory and spectra do not follow the trend of stepwise photobleaching from red to blue as expected in a simple 5-FRET system. Instead, a much more dynamic behavior is observed. In addition to spectral jumps backward and forward, the spectra are also composed by several peaks indicating that emission does not proceed from only one chromophore at the time and evidencing the presence of energy leaks in the wire and inefficient energy transfer between neighboring fluorophores. The latter is also consistent with single-molecule excited state lifetime measurements in which the lifetime of one or more donor dyes is not fully quenched upon FRET to the last dye. In fact, we typically found lifetimes of 1.1−1.4 ns for the second, third, and/or fourth dye, in contrast to the expected values of 0.15−0.19 ns in case of an efficient FRET process.[17]

TABLE 1: Extent of Energy Transfer for 75 Individual Wires

emitting dye	spectral region, nm	% molecules
second: TMR	550−600	20
third and fourth: ATTO590 and ATTO620	601−670	64
fifth: ATTO680	671−750	16

From spectral traces of 75 wires with emission maximum above 585 nm, we identified 16% of the wires emitting from the last dye. Table 1 shows the extent of energy transfer on all wires investigated. Clearly, efficient FRET occurs until the fourth dye, while a remarkable drop of emission from the fifth dye has been observed. Thus, 20% of the energy is transferred to the second dye, 64% to the third and fourth dyes, and only 16% to the fifth dye. To rule out the possibility of a less favorable FRET process occurring between the fourth and the fifth dyes, we replaced the fourth dye by other fluorophores with similar spectral properties. However, no increase in emission of the fifth dye was observed in the new constructs, suggesting that the spectral overlap between the last two dyes cannot account for the observed decrease in FRET efficiency and indicating that the major bottleneck in the FRET process occurs after the fourth dye.

We also investigated whether the low percentage of wires emitting from the last dye was due to enhanced photobleaching of the fifth dye being promoted by charge transfer along the DNA wire.[18] To that end, we recorded the number of photon counts detected before photobleaching for wires under direct excitation of ATTO680 and compared those values with the ones of the 20bp oligomer containing solely ATTO680. The results are shown in Figure 3. Both distributions can be well-fitted to single exponentials rendering values of $(2.2 \pm 0.4) \times 10^4$ and $(1.7 \pm 0.4) \times 10^4$ counts for the wire and oligomer, respectively. Similar values were also obtained for the wires showing emission from the last dye under excitation of RhG, the first dye of the chain. The similarity of the number of photon

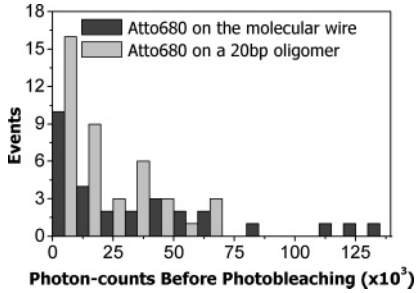

Figure 3. Histogram of the number of photon counts detected before photobleaching for DNA wires under direct excitation of ATTO680. Superimposed in the same histogram, the photon counts before photobleaching of a 20bp oligomer containing solely ATTO680 are shown.

counts obtained in all cases allows us to rule out premature photobleaching as the main source for the low emission of the wire from the fifth dye. Similar investigations for dyes at position 3 and 4 were not possible due to larger spectral overlap, making further comparison rather difficult. Nevertheless, the spectral overlap between third, fourth, and fifth dyes is such that even if the fourth dye is irreversibly photobleached, FRET from the third to the fifth dye with an efficiency of 56% is still expected (average distance of 6.8 nm). Furthermore, we designed wires with different dye combinations (RhG-TMR-ATTO590-LCR-ATTO680; RhG-TMR-Cy3.5-LCR-ATTO680, and RhG-TMR-ATTO590-ATTO647-Cy5.5), and no FRET improvement from the original design was obtained, consistent with our observations that the intrinsic photophysical properties of the dyes and their photostability are not the main cause of the low percentage of wires exhibiting high FRET until the last dye.

These observations suggest that the bottleneck on the FRET process occurring in DNA wires might reside on the structural properties of the scaffold and/or its interaction with the glass substrate, i.e., incomplete hybridization until the last dye and/or conformation freedom of the wire. In particular, the latter would result in an effective increase of the distance between the dyes and/or unfavorable dipole orientation, reducing the overall extent of energy transfer. To enquire on the degree of DNA hybridization at the single-molecule level, we performed PIE experiments with a time-resolved confocal fluorescence microscope MicroTime200 (PicoQuant).[16] The technique consists of a multicolor pulsed interleaved excitation scheme together with spectrally separated multichannel detection that allows tracking of the excitation origin of each detected photon. In our approach we used two pulsed lasers as excitation sources ($\lambda = 468$ nm (blue) and $\lambda = 635$ nm (red)) combined with a two channel detection schemes based on time-correlated single-photon counting (TCSPC) (see Experimental Section for details). The blue laser pulse excites mainly the first dye of the molecular wire (RhG), while the red laser pulse excites only the last two dyes ATTO620 and ATTO680 with efficiencies of 75 and 40%, respectively. The fluorescence photons are split onto two spectral windows and sent to two different detectors. From the APD signals upon blue and red excitation we generated three different single-molecule images. An example is shown in Figure 4. The spots in Figure 4a correspond to wires excited by the blue laser whose emission essentially arises from the first two dyes (RhG and/or TMR). Figure 4b corresponds to wires excited by the blue laser with dominant emission from the last two dyes (ATTO620 and/or ATTO680). Finally, Figure 4c corresponds to excitation with the red laser with predominant emission from ATTO620 and ATTO680. As such, the three combined images

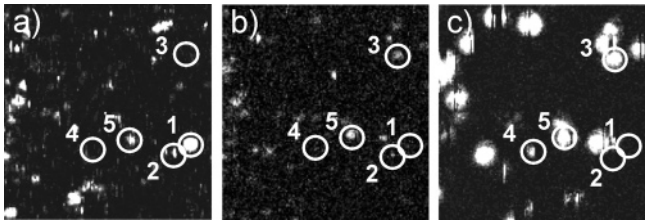

Figure 4. Pulse interleaved excitation (PIE) images of individual photonic wires (8×8 μm^2). (a) Fluorescence emission in the blue window of the spectrum (500−590 nm) upon pulsed blue excitation. (b) Fluorescence emission in the red window of the spectrum (650−720 nm) upon blue excitation. (c) Fluorescence emission in the red window of the spectrum (650−720 nm) obtained upon pulsed red excitation.

TABLE 2: Molecular Subpopulations As Obtained from PIE Images

group	excitation	emission	%
1	Blue	blue	40
2	Blue	blue/red	26
3	Blue	red	13
4	red	red	11
5	Blue/red	blue/red	10

provide valuable information about the quality of the device and the integrity of the DNA scaffold.

From 356 fluorescence spots analyzed over different sets of images we could identify five different subpopulations of molecules according to their excitation/emission characteristics. Some examples are shown in Figure 4, with the subgroups being denoted from 1 to 5. Group 1 corresponds to molecules which showed emission only on the first image, i.e., blue emission; group 2 exhibited emission on the first two images, i.e., blue and red emission; group 3 appeared on the last two images, i.e., red emission; group 4 exhibited emission only on the last image; and finally, group 5 corresponds to molecules that showed emission on all three images. Table 2 summarizes the results, including the percentage of molecules belonging to each subgroup. We interpret this heterogeneous behavior as follows. Group 1 should correspond to a combination of nonhybridized RhG attached to the wire and some emission from TMR as a result of the first FRET step (RhG-TMR). Group 2 corresponds most probably to molecules that exhibit FRET until the third dye, but, however, lacks the fourth and fifth dyes (absence of signal on the third image). Group 3 is formed by those wires which exhibit FRET until the fourth and/or fifth dye. Group 4, on the other hand, would most probably correspond to the fraction of nonhybridized ATTO680 (fifth dye) and/or the lack of RhG (first dye) on the wire, which completely prevents FRET. Finally, group 5 is composed by the fraction of wires that exhibit FRET until the last dye but accompanied by multiple energy leaks or less efficient energy transfer among neighboring fluorophores. The existence of the latter is also consistent with the spectral data already described where a complex superposition of spectral peaks from individual dyes on the wire was observed.

As such, the results obtained by the PIE experiments evidence the large heterogeneity of DNA-based photonic wires. Thus, 77% of the molecules do not work as expected. This is most probably due to incomplete hybridization until the last dye, the formation of secondary structures, and possibly interactions with the surface. Furthermore, from the remaining 23% of the wires fully hybridized, approximately half of them exhibit multiple pathways for their emission (group 5) as evidenced from their emission being recorded in the three images shown in Figure 4.

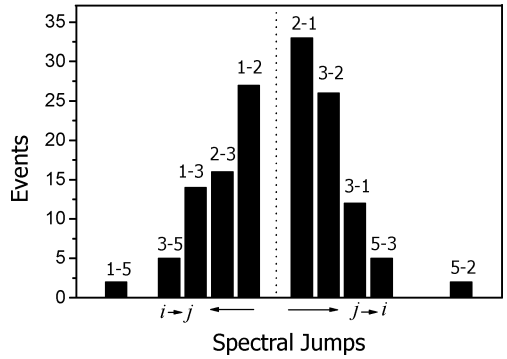

Figure 5. Spectral jumps histogram obtained from 36 single-molecule time traces. The dyes on the wire are numbered from 1 to 5: 1 for RhG, 2 for TMR, 3 for ATTO590 and ATTO620, and 5 for ATTO680. Spectral jumps are denoted as $i-j$ and indicate a jump from the ith dye toward jth dye. For instance jump 5−3 means a spectral jump from the fifth dye to the third dye.

Photon emission from multiple dyes results from an inefficient FRET process brought about by unfavorable distances, spectral overlap, and/or dipole orientation between adjacent donor−acceptor pairs and/or unexpected spectral jumps between the dyes. In fact, we observed abrupt and random spectral changes from our trajectories, as already illustrated in Figure 2. We have studied in detail the back and forth spectral jumps occurring on individual wires. For every spectral trajectory we recorded each separate jump of the peak maximum of the emission spectrum by taking into account its spectral position before and after a jump; i.e., jump $i-j$ corresponds to a spectral jump from dye i to dye j. Figure 5 shows the histogram of all spectral jumps obtained in this way.

Surprisingly, we obtain a rather symmetric histogram, indicating that the occurrence probability of jump $i-j$ is comparable to jump $j-i$. In a simple, unidirectional single-molecule FRET process, a spectral jump is only expected upon photobleaching of the lower energy emitting dye, i.e., jumps from $j \rightarrow i$, where j is always lower in energy than i. We believe that the symmetric spectral jump distribution found in our case is a signature of the existence of kinks on the double DNA helix due to the loss of covalent bonds in the positions where the dyes are attached to the DNA scaffold. The presence of those kinks would essentially reduce the rigidity of the wire changing effectively the distance and orientation between the dyes and affecting FRET. Those kinks might be mobile, and thus sudden and random spectral changes would be observable. In addition, the attachment of the wires to the glass surface might also induce occasional rotational jumps, altering the dipole−dipole coupling between adjacent dyes and resulting in the spectral jumps observed. Finally, we cannot rule out spectral diffusion of the dyes on their own[19] as an additional source for variations in the spectral overlap between adjacent donor−acceptor pairs that could be responsible for multiple dye emission.

Conclusions

We have performed bulk and single-molecule experiments on DNA-based molecular photonic wires, demonstrating energy transfer over 13.6 nm in space and more than 200 nm in spectral range from the initial donor to the final acceptor. While on fully intact wires energy transport close to 100% has been achieved, conformational freedom of the wire and partial DNA hybridization lead to multiple pathways for the photon emission on individual constructs. The use of DNA ligase enzymes after hybridization should help to improve the rigidity of the wires by repairing the missing covalent bonds occurring during the labeling process. Moreover, the use of new labeling strategies that fix not only the distance but also the orientation between the chromophores would be the next step in order to increase the efficiency and extend the transfer of energy beyond five molecules and build up longer molecular wires. Noticeably, the refined photophysical understanding of this molecular array has only been possible by our approach of combining SMS together with PIE. We believe that the combination of both techniques opens up a new way to understand and characterize the functional photophysics of other relevant and more complex systems in the emerging field of molecular photonics.

Acknowledgment. This work has been supported by the EC Program IHP-99 (Grant HPMF-CT-2002-01698) and the MCyT Program Ramon y Cajal (J.H.), VW-Stiftung (M.H.), and FOM (G.S-M, E.M.H.P.v.D.).

References and Notes

(1) (a) Yasutomi, S.; Morita, T.; Imanishi, Y.; Rimura, S. *Science* **2004**, *304*, 1944. (b) Moresco, F.; Meyer, G.; Rieder, K.-H.; Tang, H.; Gourdon, A.; Joachim, C. *Phys. Rev. Lett.* **2001**, *86*, 672.

(2) (a)Wagner, R. W.; Lindsey, J. S.; Seth, J.; Palaniappan, V.; Bocian, D. F. *J. Am. Chem. Soc.* **1996**, *118*, 3996. (b) Holten, D.; Bocian, D. F.; Lindsey, J. S. *Acc. Chem. Res.* **2002**, *35*, 57.

(3) (a) Feringa, B. L.; van Delden, R. A.; Koumura, M.; Geertsema, E. M. *Chem. Rev.* **2000**, *100*, 1789. (b) Feringa, B. L. *Acc. Chem. Res.* **2001**, *34*, 504.

(4) (a) Irie, M.; Fukaminato, T.; Saski, T.; Tamain, N.; Kawai, T. *Nature* **2002**, *420*, 759. (b) Heilemann, M.; Margeat, E.; Kasper, R.; Sauer, M.; Tinnefeld, P. *J. Am. Chem. Soc.* **2005**, *127*, 3801. (c) Habuchi, S.; Ando, R.; Dedecker, P.; Verheijen, W.; Mizuno, H.; Miyawaki, A.; Hofkens, J. *Proc. Natl. Acad. Sci. U.S.A.* **2005**, *102*, 9511.

(5) Hugel, T.; Holland, N.; Cattani, A.; Moroder, L.; Seitz, M.; Gaub, H. E. *Science* **2002**, *296*, 1103.

(6) (a) Tinnefeld, P.; Heilemann, M.; Sauer, M. *ChemPhysChem* **2005**, *6*, 217. (b) P. Tinnefeld, P.; Sauer, M. *Angew. Chem.* **2005**, *117*, 2698; *Angew. Chem., Int. Ed.* **2005**, *44*, 2642. (c) Garcia-Parajo, M. F.; Hernando, J.; Sanchez-Mosterio, G.; Hoogenboom, J. P.; van Dijk, E. M. H. P.; van Hulst, N. F. *ChemPhysChem* **2005**, *6*, 819.

(7) Heilemann, M.; Tinnefeld, P.; Sanchez-Mosteiro, G.; Garcia-Parajo, M. F.; van Hulst, N. F.; Sauer, M. *J. Am. Chem. Soc.* **2004**, *126*, 6514.

(8) Hernando, J.; de Witte, P. A. J.; van Dijk, E. M. H. P.; Korterik, J.; Nolte, R. J. M.; Rowan, A. E.; Garcia-Parajo, M. F.; van Hulst, N. F. *Angew. Chem.* **2004**, *116*, 4137; *Angew. Chem., Int. Ed.* **2004**, *43*, 4045.

(9) Kim, Y. H.; Jeong, D. H.; Kim, D.; Jeoung, S. C.; Cho, H. S.; Kim, S. K.; Aratani, N.; Osuka, A. *J. Am Chem Soc.* **2001**, *123*, 76.

(10) Ambroise, A.; Kirmaier, C.; Wagner, R. W.; Loewe, R. S.; Bocian, D. F.; Holten, D.; Lindsey, J. S. *J. Org. Chem.* **2002**, *67*, 3811.

(11) Seeman, N. C. *Nature* **2003**, *421*, 427.

(12) Hannah K. C.; Armitage, B. A. *Acc. Chem. Res.* **2004**, *37*, 845.

(13) Vyawahare, S.; Eyal, S.; Mathews, K. D.; Quake, S. R. *Nano Lett.* **2004**, *4*, 1035.

(14) Mueller, B. K.; Zaychikov, E.; Braeuchle, Ch.; Lamb. D. C. *Biophys. J.* **2005**, *89*, 3508.

(15) Hernando, J.; van der Schaaf, M.; van Dijk, E. M. H. P.; Sauer, M.; García-Parajó, F. M.; van Hulst, N. F. *J. Phys. Chem. A* **2003**, *107*, 43.

(16) (a) Ruettinger, S.; Kraemer, B.; Roos, M.; Hildt, E.; Koberling, F.; Macdonald, R. *J. Biomed. Opt.*, in press. (b) Wahl, M.; Koberling, F.; Patting, M.; Rahn, H.; Erdmann, R. *Curr. Pharm. Biotechnol.* **2004**, *5*, 299.

(17) Andrew, P.; Barnes, W. L. *Science* **2000**, *290*, 785.

(18) Dietrich, A.; Buschmann, V.; Mueller, C.; Sauer, M. *Rev. Mol. Biotechnol.* **2002**, *82*, 211.

(19) Xie, X. S.; Trautman, J. K. *Annu. Rev. Phys. Chem.* **1998**, *49*, 441.